

Prediction of the Launch Pulse for Gas-Generator-Launched Missiles

C. T. Edquist*

Martin Marietta Astronautics Group, Denver, Colorado 80201

The small intercontinental ballistic missile (SICBM) is launched using a cool gas launch eject system similar to those used for Peacekeeper and submarine-launched missiles. The SICBM system is unique in that a methanol/water mixture is used as coolant. A model of the breech fluid dynamics for predicting the launch pulse has been developed and verified with Peacekeeper data. In order to apply the model to the SICBM, the thermodynamic data for aqueous solutions of methanol of arbitrary composition have been studied and the necessary information developed. This paper describes the launch model and gives comparisons of the predicted launch pulses with both Peacekeeper and SICBM test data.

Nomenclature

A = area
 a = acceleration
 C_d = discharge coefficient
 c_f = coefficient of friction
 d = diameter
 E = energy
 F = force
 f = coolant to propellant flow-rate ratio
 g_c = standard gravity
 H = enthalpy
 h_c = heat-transfer coefficient
 J = mechanical equivalent of heat
 L_s = seal length
 M = Mach number
 m = mass
 \dot{m} = mass flow rate
 Pr = Prandtl number
 p = pressure
 Q = heat lost
 q = heating rate
 R = gas constant
 Re = Reynolds number
 T = temperature
 t = time
 U = internal energy
 v = velocity
 W = work done
 w = weight
 x = distance
 β = coolant flow-rate parameter
 γ = isentropic exponent
 θ = angle
 μ = viscosity
 ρ = density

Subscripts

a = ambient or air
 b = base
 c = coolant or canister
 e = edge
 f = friction
 g = gas generator

i = in
 L = launch
 l = liquid
 m = missile
 o = out or $t = 0$
 p = propellant
 r = breech
 s = seal
 t = tube

Introduction

THE loads incurred during the launch phase of a canister-launched missile may exceed those experienced in flight. The launch phase must be thoroughly analyzed to predict these loads accurately. Both self-eject and gas-generator launch techniques are possible, and the gas generator concept can be further divided into hot and cool gas procedures. With the hot gas generator (HGG) method,¹ a rocket motor is fired in the breech below the missile, and the resultant pressurization forces the missile out. The cool gas concept adds a liquid coolant chamber and mixing region between the HGG and the breech, and the propellant products partially vaporize the coolant. The resulting mixture remains relatively cool, i.e., below supersaturation temperatures as long as sufficient coolant is supplied. The cool gas system leads to a less severe environment for equipment in the missile base region. The launch eject system (LES), i.e., the rocket motor and coolant mixing device, is insensitive to breech pressure and operates essentially independently of the conditions in the launch tube. The details of its operation have been considered elsewhere.² Assuming this independence between the LES and the breech, the requirements for prediction of the launch pulse are a knowledge of the HGG chamber pressure history, the propellant and coolant properties, eject system flow areas, and missile and launch tube physical characteristics. A schematic of the problem considered is shown in Fig. 1.

Analysis

Basic Equations

The basic equations required for the solution of a missile launch from a canister are the conservation of mass and energy, the equation of vehicle motion, and an equation of state for the fluid in the breech. The present approach uses the integral forms of the conservation relations which are

$$m_r = m_{r_0} + \int_0^t (\dot{m}_i - \dot{m}_o) dt \quad (1)$$

$$U_r = U_{r_0} + E_i - E_o - Q - W$$

Presented as Paper 88-3290 at the AIAA/ASME/SAE/ASEE 24th Joint Propulsion Conference, Boston, MA, July 11-13, 1988; received Jan. 6, 1989; revision received Aug. 25, 1989; accepted for publication Aug. 25, 1989. Copyright © 1990 by the American Institute of Aeronautics and Astronautics, Inc. All rights reserved.

*Senior Staff Engineer. Senior Member AIAA.

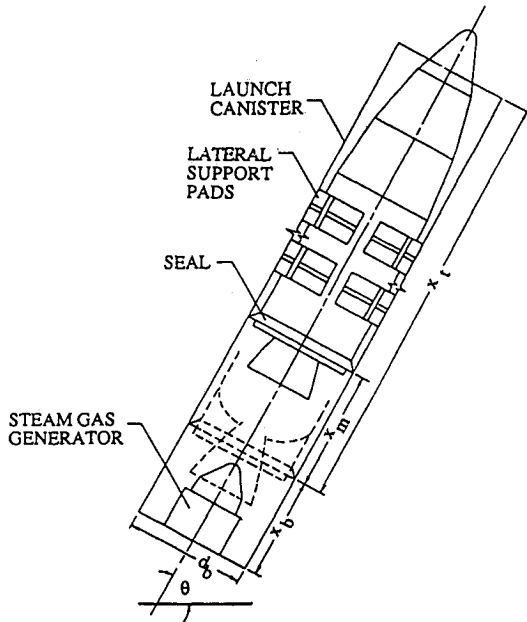


Fig. 1 Canister launched missile schematic.

where

$$E_i = \int_0^t (\dot{m}_p H_p - \dot{m}_c H_c) dt \quad (2)$$

$$E_0 = \int_0^t (\dot{m}_{a_0} H_{a_r} + \dot{m}_{p_0} H_{p_r} + \dot{m}_{c_0} H_{c_r}) dt$$

$$Q = \int_0^t qA dt$$

$$W = \frac{A_t}{J} \int_0^t p_r v_m dt \quad (3)$$

The vehicle motion is described by

$$w_m a_m = (p_r - p_a) A_b - F_f - w_m \sin \theta_L \quad (4)$$

with

$$v_m = g_c \int_0^t a_m dt$$

$$x_m = \int_0^t v_m dt \quad (5)$$

Evaluation of Eqs. (3) is straightforward once the geometry of the situation is known, the HGG operating characteristics are defined, and propellant and coolant are well characterized thermodynamically. Instantaneous and complete mixing of ambient, propellant, and coolant constituents is assumed with mass averaged properties and no chemical reactions. At any time, the properties are uniform throughout the breech. The gases are assumed to obey Dalton's law of partial pressures, and the liquid and gas phases of the coolant are taken to be at saturation. The ambient gas is characterized by a single value of the isentropic exponent and gas constant.

Propellant Properties

The gas-generator chamber temperature can be found from the known propellant formulation using established computer codes.³ Though a weak function of chamber pressure, the usually quoted chamber temperature values correspond to 1000 psia. Also required is the isentropic exponent and the

propellant gas constant. Selection of these values is important as they directly affect the energy input for the problem. As a consistent and reasonable choice, values found by an equilibrium isentropic expansion from chamber temperature and 1000 psia to sonic conditions are used. These HGG throat conditions occur just prior to the coolant/hot gas interaction.

Coolant Properties

The coolant thermophysical properties required are the saturation pressure, the heat of vaporization, the liquid and vapor saturated densities, specific heats and enthalpies, and the saturated vapor internal energy, all as a function of temperature. For water, the Peacekeeper coolant, these properties are readily available.⁴ The operational requirements for the small intercontinental ballistic missile (SICBM) dictate a coolant with a freezing point below 0°F. The theoretical treatment of the properties of solutions has been well described,⁵ and those procedures have been applied to the aqueous solutions of methanol. The resulting analysis was used to develop the requisite properties for a 27.1% methanol (by volume) solution, the coolant selected for the SICBM LES.

Energy In

The control volume used in the analysis procedure excludes the hot gas generator and coolant chamber. That is, these supply only input energy and mass and the energy losses and fluid changes in the LES are not modeled. The mass addition to the breech can be determined in three ways: both propellant and coolant flow rates can be input from a separate LES analysis; the propellant flow rate can be specified and the coolant values subsequently calculated; or the HGG chamber pressure can be input and both propellant and coolant flow rates calculated therefrom. For the latter case there is, neglecting the effect of gravity in the coolant chamber and for $M \geq 1$,

$$\dot{m}_p = (C_d A)_g P_g \left[\left(\frac{2}{\gamma + 1} \right)^{\frac{\gamma + 1}{\gamma - 1}} \frac{\gamma}{RT} \right]_g^{\frac{1}{2}}$$

$$\dot{m}_c = (C_d A)_c (2 \rho_l \Delta p_c)^{\frac{1}{2}} \quad (6)$$

Defining the parameter β as

$$\beta = \frac{\dot{m}_c}{\dot{m}_p^{\frac{1}{2}}} \quad (7)$$

then

$$\beta = \left[\frac{4 \left(\frac{\gamma + 1}{2} \right)^{\frac{\gamma + 1}{\gamma - 1}}}{\gamma} RT \right]^{\frac{1}{4}} \frac{(C_d A)_c}{(C_d A)_g^{\frac{1}{2}}} \left(\rho_l \frac{\Delta p_c}{p_g} \right)^{\frac{1}{2}} \quad (8)$$

For a given propellant and coolant, β depends primarily on the effective flow areas at the HGG throat and coolant injector. This occurs since the pressure difference (Δp_c) across the coolant chamber is directly proportional to the HGG chamber pressure (p_g). The proportionality constant depends on the design of the LES system. With given flow areas, β is, to good approximation, constant during the launch pulse. Given an HGG propellant flow rate, the coolant flow rate in the absence of detailed analysis is then given by Eq. (7). The minimum ratio of coolant to propellant flow rate thus occurs at the maximum propellant flow rate, and the eject system is designed to a given value of this ratio, i.e.,

$$f = \left(\frac{\dot{m}_c}{\dot{m}_p} \right)_{\max} = \frac{\beta}{\dot{m}_p^{\frac{1}{2}}_{\max}} \quad (9)$$

Having determined the mass entering the system, the energy into the system can be determined to a first approximation by assigning constant values to the propellant and coolant enthalpies in Eqs. (3). The propellant value is determined as just mentioned, whereas the coolant value is the liquid value at the

ambient temperature. If the LES is designed for minimum weight, then the coolant may heat during the launch pulse, and the coolant energy into the system should reflect that temperature rise. Coolant heating did not occur for the Peacekeeper, however, for the SICBM significant heating does occur late in the pulse, and this is included in the model.

Energy Lost

Mass and its accompanying energy are lost out of the system past the launch seal (see Fig. 1). This loss is described by assigning an effective leakage area (from empirical data) past the seal. The mass and energy losses are then a function of this area and the pressure difference across the seal.

The high energy and velocity fluid in the breech leads to significant heat transfer to the tube walls and base, the missile base, and HGG components in the breech. This heating is relatively simply described in the present model. A two-phase heat-transfer coefficient for flow up a wall⁶ is used for the heating to the breech and tube components. This is

$$h_{c_r} = 0.065 u_e \left(\rho_l \rho_r \frac{c_f}{Pr} \right)^{1/2} \quad (10)$$

with

$$c_f = \frac{1.957}{[\ln(Re_r)]^{2.58}} \quad (11)$$

and

$$x_g = x_r + x_m \quad (12)$$

A turbulent gas phase relation is used in the vehicle base region and is given by

$$h_{c_b} = \frac{0.0360}{Pr^{0.533}} \frac{\mu}{x_b} Re_b^{4/5} \quad (13)$$

with

$$x_b = d_b/2 \quad (14)$$

The effective boundary-layer edge velocity is determined from the momentum of the entering fluid imparting a circulation to the breech fluid.¹ The length scales are also geometry dependent and the tube value varies through the launch pulse. With the heat-transfer coefficient defined, a one-dimensional slab conduction analysis provides the surface temperature and heat loss considering breech, base and tube areas, and their separate materials independently.

Friction Force

The model describing the friction⁷ assumes it to be composed of two components, that due to the pads and that due to the seal. The pad friction is composed of two parts. First, if the pads must be compressed to insert the vehicle into the canister, each pad will exert a normal force with resultant friction. As the vehicle moves up the canister during launch, the pads attached to the vehicle leave the canister, and the total friction is reduced. The pad location and contact area must be specified to monitor these variations. Second, for launch angles other than vertical, the vehicle weight acting on the pads causes friction. This component is independent of the pad area in contact with the launch tube.

The launch seal also contributes to the friction force and is a function of the seal geometry and the pressure differential across it. The seal friction peaks at the maximum breech pressure. The relations describing the seal friction are

$$F_{f_s} = \frac{c_{f_s'}}{c_{f_s} \sin \theta_s + \cos \theta_s} [F_c \cos \theta_s + kP] \quad (15)$$

with

$$\sin \theta_s = \frac{R_c - R_m}{L_s}$$

$$k = \frac{\pi}{6 \sin \theta_s} (2R_c + R_m)(R_c - R_m) \quad (16)$$

Launch Pulse

The launch pulse is found by a simple time-marching procedure for Eqs. (1-5) from the known initial conditions. To determine the breech thermodynamic state, the mass and internal energy at each time step are found from the conservation equations. An estimate of the breech temperature is made and an iteration performed until the resultant internal energy meets the prescribed criterion. The vehicle acceleration is then found from the equation of motion. Its solution requires the pressure difference acting on the vehicle and knowledge of the restraining friction force. With the acceleration determined, the vehicle velocity and displacement result from the preceding integrations [see Eqs. (5)], providing a new breech volume. The calculation proceeds until the seal passes the lip of the canister. If desired, an approximate canister blowdown calculation can be made by using the prescribed leakage area to approximate the opening of the canister mouth as the vehicle skirt and nozzle pass by. The launch pulse calculation in this case continues until the vehicle stops accelerating.

Results

Peacekeeper

The most complete data available for steam launch pulses are those from the Peacekeeper Canister Assembly and Launch Test Program (CALTP) tests. In particular, the Minuteman Upper Silo Simulation (MMUSS) series of four tests was well instrumented for launch pulse examination. Three axis missile accelerations were measured as well as pressures and temperatures at a number of locations within the breech. The data have been used extensively to examine seal leakage, muzzle blast, and pad release phenomena.⁸ MMUSS-1 and -2 used a composite material launch tube and compressed lateral support pads such that significant pad friction was generated during the launch pulse.⁷ For MMUSS-3 and -4, a larger diameter steel canister was used so that no pad compression was required. This resulted in a much lower friction force composed primarily of seal friction. In addition the overall data retrieval seemed more successful for MMUSS-3 than MMUSS-4. For these reasons, the data from MMUSS-3 have been used to calibrate the present model.

Figure 2 compares MMUSS-3 axial acceleration data with calculations. First, note the curve identified as 100% energy. This variation results from application of the present model with data directly from the test report and known physical

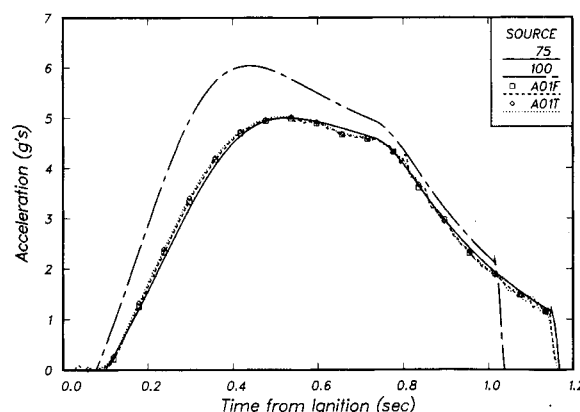


Fig. 2 Effect of propellant energy on MMUSS-3 missile acceleration.

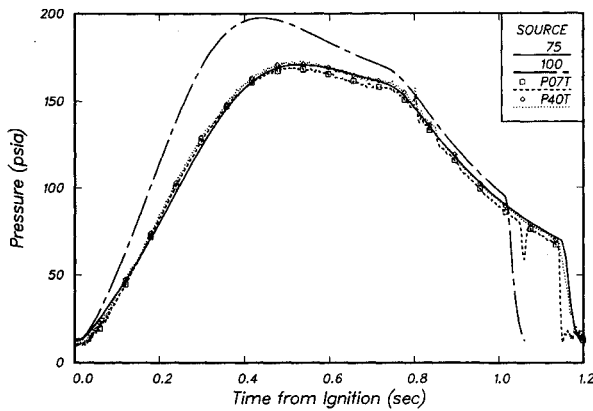


Fig. 3 Effect of propellant energy on MMUSS-3 breech pressure.

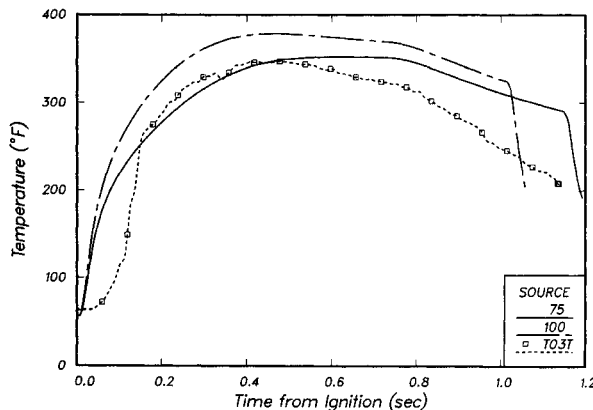


Fig. 4 Effect of propellant energy on MMUSS-3 breech temperature.

data. The acceleration is overpredicted as is the breech pressure presented in Fig. 3 and the temperature displayed in Fig. 4. In light of the preceding discussion of propellant properties and also since the details of the internal LES operation are not considered, a factor less than one was applied to the incoming propellant energy, not the mass flow rate. After some iteration, a factor of 0.75 was chosen as providing the best match with test data as seen in the same figures where the agreement with the test data is excellent. This factor represents the propellant energy remaining in the propellant mass after traveling through the LES hardware. The lost energy is reflected in increased hardware and coolant temperatures and is not usually recovered during the launch pulse.

For these results, the propellant flow rate was calculated from the measured chamber pressure and the coolant flow rate then found by specifying the parameter β . Each of the preceding three coolant flow-rate calculations was tried. Although each method adequately represents the launch pulse, the best overall fit to the data was provided by the simplest flow-rate calculation derived from the chamber pressure and coolant flow-rate correlation.

Using the pressure-based flow-rate calculation and retaining the 75% propellant energy factor, the launch pulses have been calculated for all four of the MMUSS tests and compared with the available data. Axial acceleration, breech pressure, and temperature for MMUSS-1 are shown in Figs. 5-7. Corresponding graphs for MMUSS-2 are displayed in Figs. 8-10, and MMUSS-4 in Figs. 11-13. As mentioned, MMUSS-1 and -2 used a small diameter, composite canister so that friction between the pads and canister was significant. The condition of both the pad surface and interior canister surface affects the friction so that modeling the phenomena is difficult. This is evidenced in Figs. 5 and 6 where the acceleration is overpredicted for the first 0.6 s, whereas the forcing pressure is well

matched. Since the friction is the other major contributor to the acceleration pulse, it seems the present friction model is inadequate for MMUSS-1. The situation is better for MMUSS-2 with generally good agreement between analysis and data.

MMUSS-3 and -4 used a larger diameter steel canister with resulting small pad friction but still significant seal friction. Examination of the comparisons for these last two tests (see Figs. 2-4 and 11-13) indicate generally excellent agreement between analysis and data suggesting a good seal friction model. The peak acceleration and maximum breech pressure during the pulse and the missile velocity at exit are three of the most important pulse parameters. The calculated and test-derived values are compared in Table 1, where it is seen that the results are within 2% for all of the tests except for the MMUSS-1 acceleration.

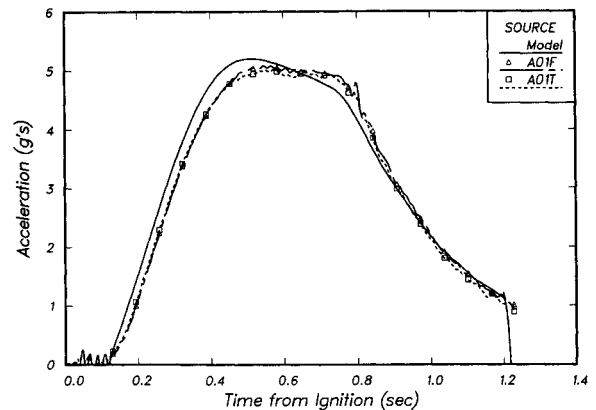


Fig. 5 Peacekeeper CALTP MMUSS-1 missile acceleration.

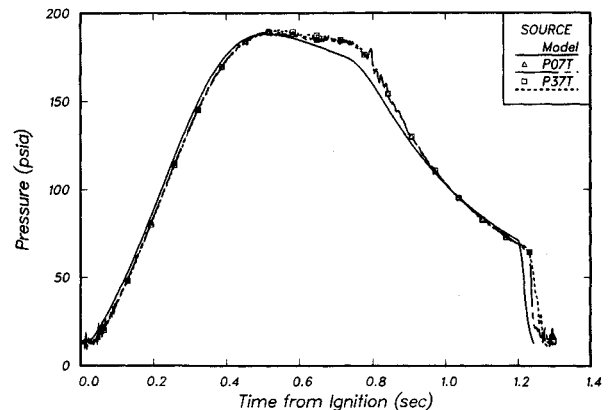


Fig. 6 Peacekeeper CALTP MMUSS-1 breech pressure.

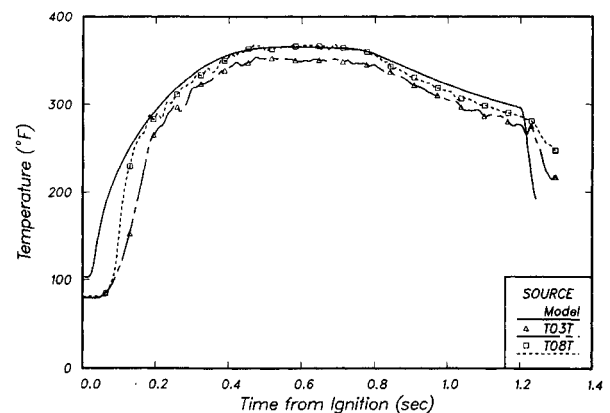


Fig. 7 Peacekeeper CALTP MMUSS-1 breech temperature.

Small ICBM

Having described the launch pulse model and its application to the Peacekeeper situation, we now address the SICBM for which this present model was developed. Although a number of tests of the SICBM LES had been conducted prior to the SICBM CALTP, none involved an actual launch. The previous tests provided information to improve the temperature correlation.⁹ Figures 14 and 15 show, respectively, the acceleration and breech pressure comparisons with the CALTP-1 data using the pre-CALTP version of the launch pulse model. Although the maximum acceleration and pressure compare reasonably well with the data, the pulse shape is not satisfactorily reproduced.

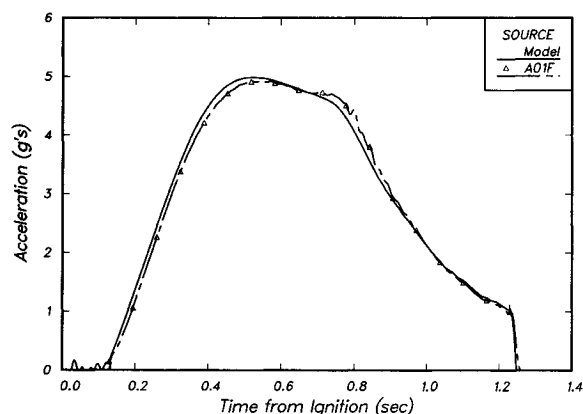


Fig. 8 Peacekeeper CALTP MMUSS-2 missile acceleration.

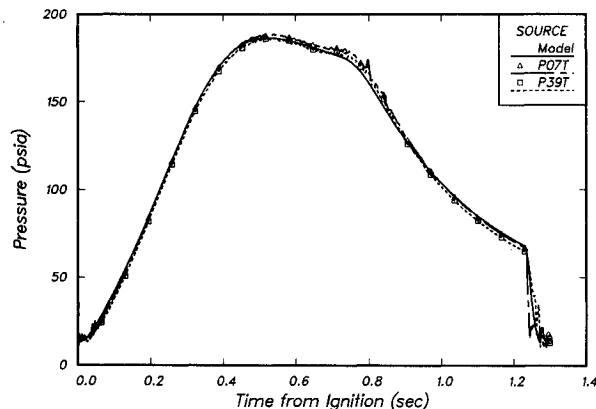


Fig. 9 Peacekeeper CALTP MMUSS-2 breech pressure.

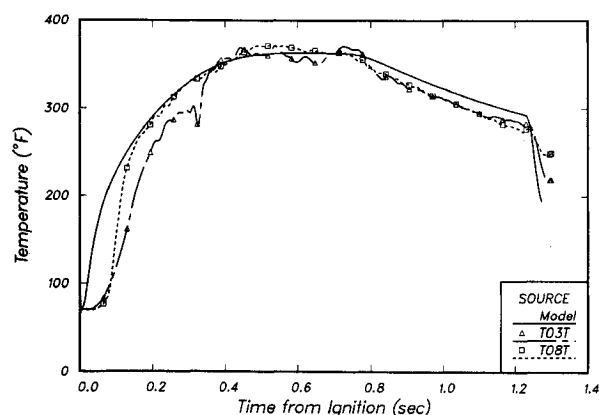


Fig. 10 Peacekeeper CALTP MMUSS-2 breech temperature.

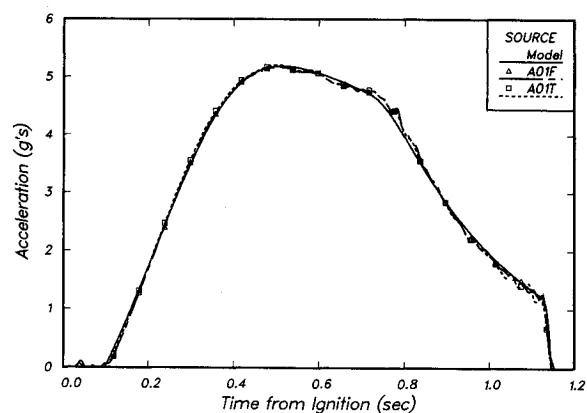


Fig. 11 Peacekeeper CALTP MMUSS-4 missile acceleration.

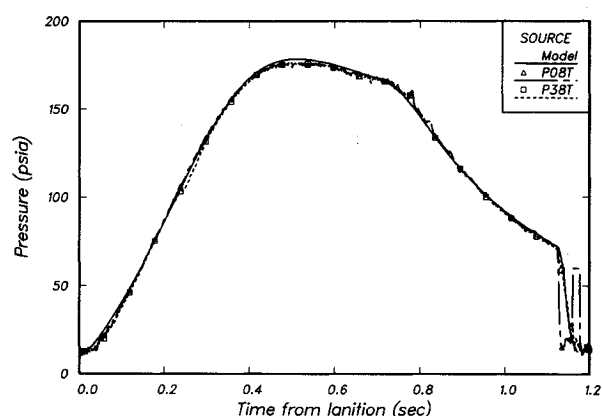


Fig. 12 Peacekeeper CALTP MMUSS-4 breech pressure.

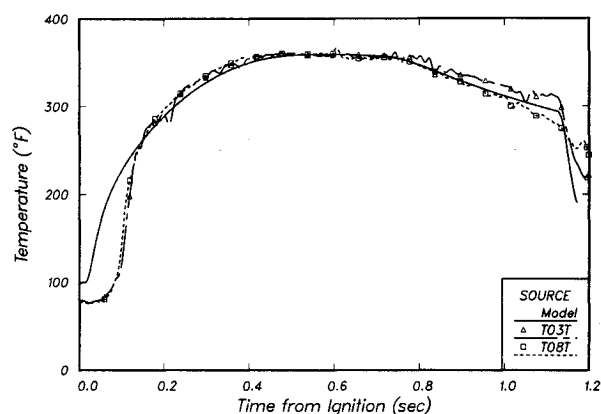


Fig. 13 Peacekeeper CALTP MMUSS-4 breech temperature.

Table 1 Comparison of calculated and measured Peacekeeper MMUSS launch pulse parameters

MMUSS test	Peak acceleration, g		Peak pressure, psia		Exit velocity, fps	
	Test	Model	Test	Model	Test	Model
1	5.0	5.2	189	188	115	117
2	4.9	5.0	186	186	114	113
3	5.0	5.0	172	170	111	110
4	5.2	5.2	175	179	112	112

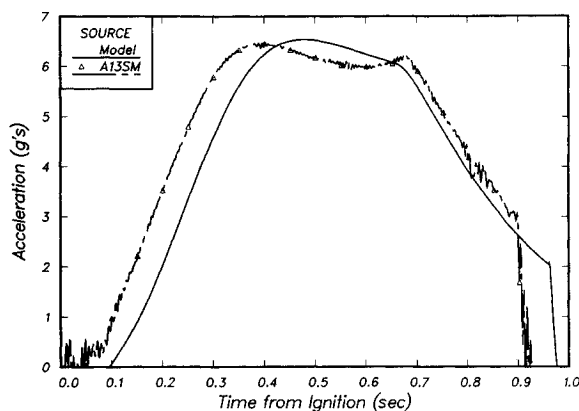


Fig. 14 SICBM CALTP-1 pretest model missile acceleration.

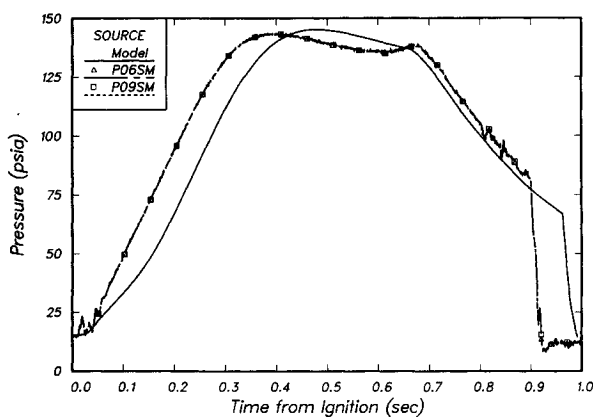


Fig. 15 SICBM CALTP-1 pretest model breech pressure.

Two regions of the pulse are of concern. First, the initial rise is much delayed, and second, the secondary peak does not appear. In order to improve the correlation, initially some modifications to the breech, launch tube, and base heating were made to better represent the actual processes that occur. These changes did not produce the results desired. An examination of the breech volume prior to missile motion reveals an extremely cluttered and disjointed arrangement. Partly because of the scale change between SICBM and Peacekeeper, the SICBM arrangement is more complex and compartmentalized than for Peacekeeper. This geometry acts as a baffle to the injected LES products, not allowing the large velocity swirling, high kinetic energy content described by the model, and with only locally high heating rates prior to missile motion. As a remedy to this problem, the kinetic energy term in the energy equation has been eliminated for the SICBM situation.

The remaining issue is the absence of a second peak to the pressure or acceleration pulse. Examination of data from the tests¹⁰ of the Simulated Breech Assembly Test (SBAT) shows that the coolant is heated by the injected propellant in the coolant chamber during operation of the LES. Figure 16¹⁰ presents the coolant temperature at various locations in the coolant chamber during the SBAT-1 test. Gauge T45LA measures the temperature near the coolant chamber outlet. The previous model assumed the injected coolant to be at ambient temperature. In addition, the model assumed only 75% of the propellant energy was active during the launch. The remaining propellant energy is lost to the coolant and the internal portions of the LES and does not contribute to the launch pulse. In refining the model, part of the lost propellant energy is now regained by heating the coolant. With the data of Fig. 16 as a guide, the injected coolant temperature is increased linearly during the time period from $0.7 t_{\max}$ to t_{\max} , the time of peak

HGG chamber pressure. The coolant temperature is held constant before and after these times at their respective levels.

With these two important changes and the propellant energy fraction now taken to be 0.74 allowing for slightly more energy lost in the LES, a comparison of the analytical results with the CALTP-1 data is given in Figs. 17–19. The correlation can be considered excellent.

Two more SICBM CALTP tests have been conducted. However, no more model changes have been introduced. The comparison of the CALTP-2 data with the present model is displayed in Figs. 20–22. The model predicts the data reasonably well, but the correlation is not as good as for CALTP-1. The temperature rise seen late in the pulse for the SICBM is

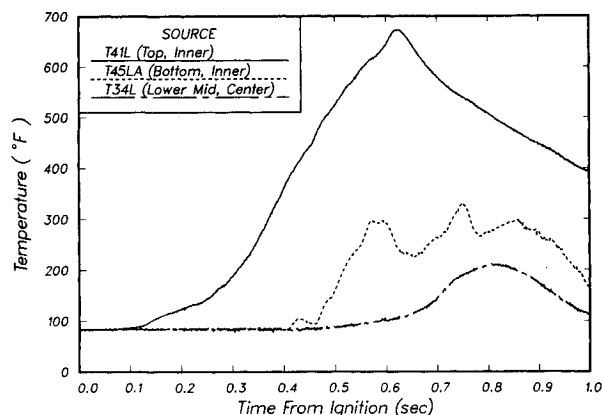


Fig. 16 SBAT-1 coolant temperatures in the chamber.

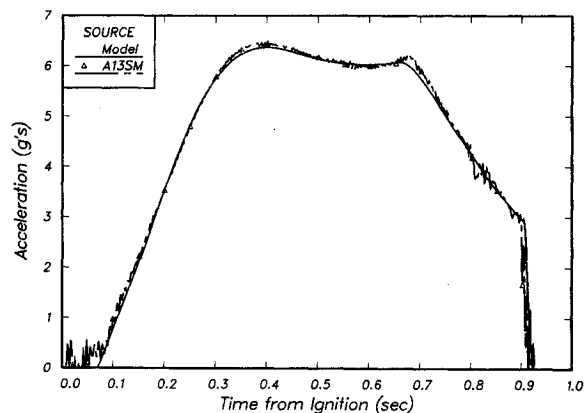


Fig. 17 SICBM CALTP-1 missile acceleration.

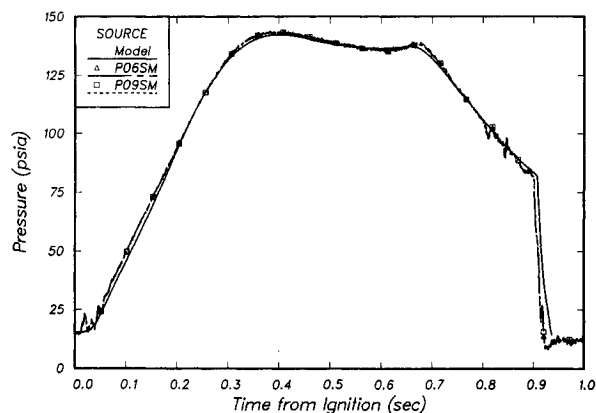


Fig. 18 SICBM CALTP-1 breech pressure.

due to local superheating near the gauge location at the LES exit. The gauges are on the missile base for Peacekeeper, and so are far up the canister at comparable times.

For the first two tests, a mass simulated missile (MSM) was used that matched the SICBM in mass and, in general, the stage I base and nozzle geometry. For CALTP-3, a ground test missile (GTM) was used for the first stage thus duplicating the SICBM as to the parts exposed to the LES. The motor case volume is larger than that for the MSM, and this leads to a somewhat altered pulse shape as seen in Figs. 23-25. The model to data correlation for CALTP-3 is, in quality, somewhere between that for the first two tests.

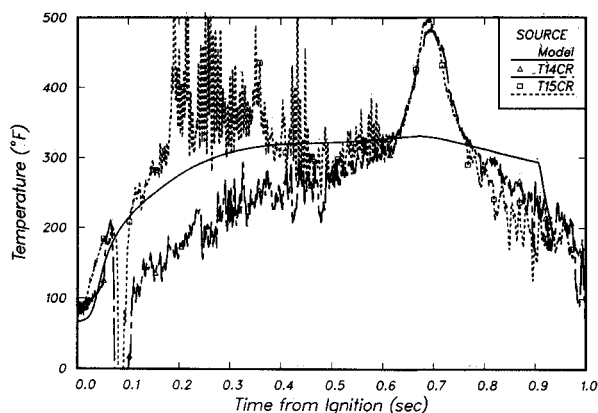


Fig. 19 SICBM CALTP-1 breech temperature.

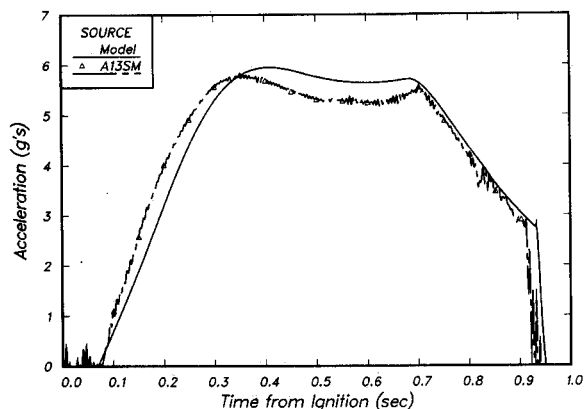


Fig. 20 SICBM CALTP-2 missile acceleration.

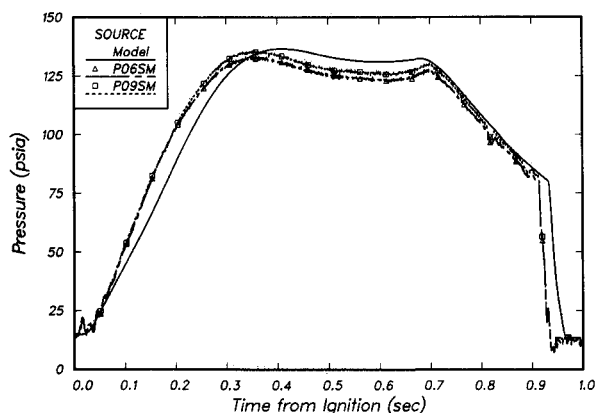


Fig. 21 SICBM CALTP-2 breech pressure.

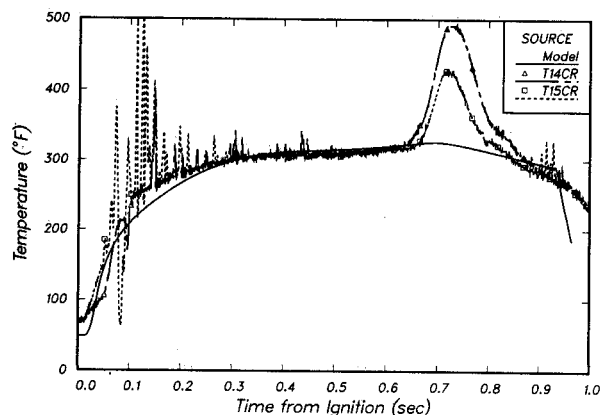


Fig. 22 SICBM CALTP-2 breech temperature.

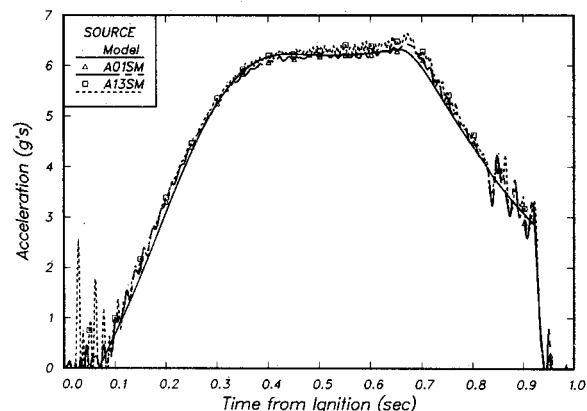


Fig. 23 SICBM CALTP-3 missile acceleration.

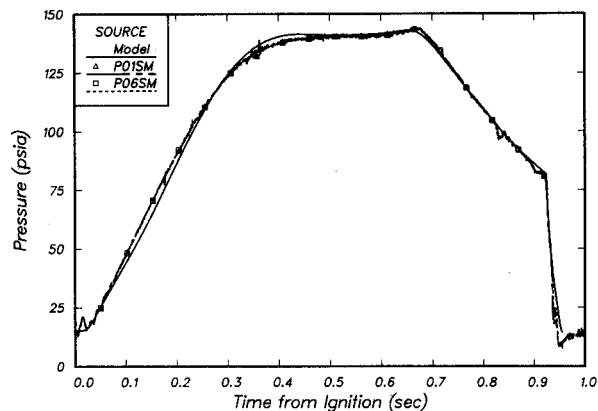


Fig. 24 SICBM CALTP-3 breech pressure.

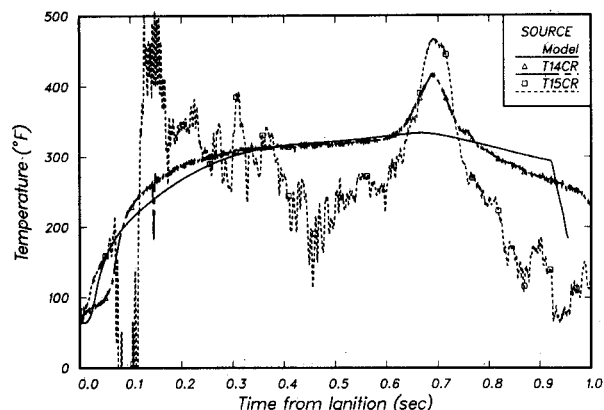


Fig. 25 SICBM CALTP-3 breech temperature.

Table 2 Comparison of calculated and measured SICBM CALTP launch pulse parameters

CALTP test	Peak acceleration, g		Peak pressure, psia		Exit velocity, fps	
	Test	Model	Test	Model	Test	Model
1	6.4	6.4	144	142	131	130
2	5.8	6.0	135	137	123	126
3	6.5	6.3	146	143	127	129

A comparison of the test-derived and calculated important pulse parameters is displayed in Table 2 for the SICBM. As with the Peacekeeper, the model predicts these test results within about 2-3% suggesting that the presently described model will adequately simulate all of the SICBM launch situations.

Summary

A gas dynamic model of the process involved in launching the SICBM from a canister has been developed. The launch method is similar to that used for the Peacekeeper missile, and data from that program have been used in establishing validity of the analysis procedure. Since a methanol/water coolant is used for the SICBM, the thermodynamic properties of that mixture have been generated for use in the launch analysis. Comparison and correlation of data from three SICBM CALTP launches with the results of the present analysis confirm the success of the model.

Acknowledgment

This work was sponsored by the Department of the Air Force, Ballistic Missile Office, under Contract F04704-85-C-0040.

References

- ¹Edquist, C. T., and Romine, G. L., "Canister Gas Dynamics of Gas Generator Launched Missiles," AIAA Paper 80-1186, June 1980.
- ²Huseman, P. G., "Gas Dynamics Analysis of the Small ICBM and Peacekeeper Launch Eject Gas Generators," 26th JANNAF Combustion Meeting, Jet Propulsion Lab., California Inst. of Technology, Pasadena, CA, 1989.
- ³Nickerson, G. R., and Coats, D. E., "A Computer Program for the Prediction of Solid Propellant Rocket Motor Performance (SPP), Volume IV," Air Force Rocket Propulsion Lab., Edwards AFB, CA, AFRPL TR-84-036, Sept. 1984.
- ⁴Keenan, J. H., Keyes, F. G., Hill, P. G., and Moore, J. G., *Steam Tables*, Wiley, New York, 1969.
- ⁵Berry, R. S., Rice, S. A., and Ross, J., *Physical Chemistry*, Wiley, New York, 1980.
- ⁶*Heat Transfer Data Book*, General Electric, May 1974.
- ⁷Villano, M. C., "Small ICBM Canister Launch Friction Model," MMC CDRL TOR MCR-86-5270, May 1986.
- ⁸Edquist, C. T., Huseman, P. G., and Cosstephens, S. D., "Summary of CALTP MMUSS Gas Dynamics Results," MMC CDRL TOR SE2-317060, Oct. 1985.
- ⁹Edquist, C. T., "SLED Modifications Derived from LES Development Tests," MMA SS-87-16-0202, Oct. 1987.
- ¹⁰Cocroft, K. H., Huseman, P. G., Adams, R. E., Getchel, D. E., and Macumber, D. W., "Small ICBM Simulated Breech Assembly Test (SBAT) Test Report LES-07," MMC CDRL MCR-87-8185, Oct. 1987.